Rare-gas precipitates in metals as quantum dots for polaritons

I. Yu. Goliney and V. I. Sugakov
Institute for Nuclear Research, Ukrainian Academy of Sciences, Prospect Nauki 47, Kiev 03680, Ukraine
(Received 28 April 2000)

A study of the optical spectra of metals containing inclusions of rare-gas precipitates of spherical shape is presented. A unique feature of this system is that rare-gas atoms inside the precipitates form a crystal lattice even at temperatures much higher than room temperature. Energy spectra of the size quantization of excitons in Xe, Kr, Ar, and Ne precipitates in Al and their manifestation in reflection spectra are calculated, taking into account polariton effects (dipole-dipole exciton interactions), spatial dispersion, and mixing of the electronic excitations of the inclusion with collective excitations of the surrounding metal (plasmons). It was shown that (i) the proximity of energies of the exciton levels and the plasmons localized on the inclusion (surface plasmons) results in a gigantic shift (up to 1 eV) of the levels of coupled excitations, (ii) the transfer of the oscillator strength from the plasmon level to the exciton levels leads to the amplification of optical transitions in bubbles by several orders of magnitude. If the energy of the surface plasmon is smaller than the energy of the surface polariton (Ar, Ne), the latter is situated inside the discrete exciton spectrum and is coupled to the discrete exciton levels. In this case the surface polariton line in the reflection spectra is broadened by a set of dips representing quantized exciton levels. In the case of Xe and Kr in Al, the energy of the surface plasmon level is larger than the energy of the surface polariton. As a result, the surface polariton is pushed out of the exciton band and manifests itself in the reflection spectrum by a very narrow dip.

I. INTRODUCTION

Excitons in low-dimensional systems (quantum wells, wires and dots) have recently been a subject of numerous and intense studies.[1,2] This interest is due to the unique features of the small-size system excitons that include large coupling energy, gigantic oscillator strength, strong nonlinearity, and short radiational lifetime. The development of the technology to manufacture low-dimensional systems is a challenging problem.

This paper presents the results of a theoretical study of excitons in small crystallites of rare-gas atoms in metals. Study of the structure of rare-gas precipitates has been carried out for the past 15 years. Rare-gas atoms introduced into a metal matrix by ion implantation or created as the result of nuclear reactions have low solubility in the metal and tend to collect into bubbles. The behavior of nanometer-sized precipitates of noble gases in materials has been studied extensively because of problems associated with the development of fusion and fission reactors.[3] Pressure inside the bubbles reaches very high values, tens and hundreds of kilobars. In these conditions, rare gases crystallize at higher temperature. High-temperature crystallization (precipitation) of rare gases in bubbles was discovered experimentally by electron and x-ray diffraction, by high-angle annular dark field scanning transmission electron microscopy.[5–7] Crystallization of Xe in Al, Ar in Al, and Kr in Cu, Ni, and Au can be mentioned as examples. Melting temperature of the rare-gas precipitates can be very high. For instance, crystallized Kr in Ni exists up to a temperature of 825–875 K, while at atmospheric pressure melting occurs at 115 K.[4] Annealing the metal with rare-gas precipitates at a temperature above the melting point of rare-gas crystallites results in an increase of the radius of the bubbles and a decrease of the pressure and therefore a decrease of the melting temperature. There were some indications that even He might be crystallized in He bubbles with the melting temperature in the range of 150–210 K.[8]

Precipitation of rare-gas atoms in irradiated metals creates a unique system that combines features of high-temperature–high-pressure rare-gas crystals interacting with free electrons of a metallic surrounding and size quantization of electronic states due to the small size of the precipitates. Optical properties of metals containing such precipitates are seldom investigated. There is a paper[9] in which the spectrum of the transmission of aluminum films with helium bubbles was measured.

The paper presented here concentrates on the optical spectra of rare-gas precipitates in metals. It will be shown that the system has unique properties and the study of electron excitations localized on the precipitates may give insight both into new optical materials and into the behavior of rare-gas crystals at high temperature and pressure. Due to the periodic spatial arrangement of rare-gas atoms in the precipitates, electronic excitations of the crystallites have collective delocalized character and are excitons. The small size of the precipitates leads to the quantization of the excitations. In fact, the considered system is an example of the quantum dots that attract so much attention nowadays. Some aspects of the low-dimensional quantization of small-radius excitons in dielectric media were studied in Refs. 10–12. The paper cited in Ref. 10 considered the properties of the hypothetical crystallite of helium atoms in a metal, while the paper cited in Ref. 11 investigated the radiation lifetime of CuCl microcrystals in a matrix of silicate glass. The present paper reports the results of calculations of the energy spectrum and the spectra of reflection of electromagnetic waves of metals containing Xe, Kr, Ar, and Ne precipitates. As will be shown for some metal–rare-gas combinations, strong resonant interaction between excitations inside the precipitate and the electronic system of the metal results in a gigantic shift of levels

of quantized excitons and localized plasmons and a significant change of the oscillator strengths of optical transitions.

II. SPECTRUM OF ELECTRONIC EXCITATIONS OF DIELECTRIC INCLUSION IN METAL TAKING INTO ACCOUNT SPATIAL DISPERSION

The determination of the energy spectrum of the excitation of dielectric inclusion in a metal requires finding nontrivial solutions of the system of Maxwell equations for the electromagnetic field and the Schrödinger equation for electronic excitations. Let us consider a spherical inclusion with the radius smaller than the wavelength of the electromagnetic field with the frequency of the resonant oscillations in the system. In this case, the Maxwell equations can be written in a quasistatic approximation. The Schrödinger equation may be substituted by the equation for the vector of the exciton polarization, which was deduced from the Schrödinger equation in the linear approximation with respect to the electromagnetic field.[13] For the rare-gas crystals, the dispersion for the excitons in the bulk is parabolic, the radius of the lowest exciton state is of order of the lattice period, and thus the excitation may be considered to be a small-radius exciton. Metal is treated as a free-electron gas of the Drude theory. As a result of the above considerations, the following set of equations for the potential of the electromagnetic field and the polarization vector inside and outside the precipitate can be written:

$$\varepsilon_\infty \Delta \varphi_1 - 4\pi \,\mathrm{div}\, \mathbf{P}_1 = 0, \tag{1}$$

$$\ddot{\mathbf{P}}_1 + \omega_0^2 \mathbf{P}_1 - \alpha \Delta \mathbf{P}_1 + \beta \nabla \varphi_1 = 0, \tag{2}$$

$$\Delta \varphi_2 - 4\pi \,\mathrm{div}\, \mathbf{P}_2 = 0, \tag{3}$$

$$\ddot{\mathbf{P}}_2 + \frac{e^2 n}{m} \nabla \varphi_2 = 0. \tag{4}$$

Here, index 1 refers to the medium inside the inclusion and index 2 refers to the metal, φ_i and $\mathbf{P}_i$ are the electric-field potential and polarization vector, $\mathbf{P}_1$ is the exciton part of the polarization of inclusion, ω_0 is the frequency of the exciton band bottom of the material inside the inclusion, ω_p is the plasma frequency of the metal, and ε_∞ is the dielectric constant of the rare-gas crystal accounting for the contribution into the polarization of all states except the exciton band under consideration, $\beta = \omega_{\mathrm{LT}} \omega_0 \varepsilon_\infty / 2\pi$, where $\hbar \omega_{\mathrm{LT}}$ is the transverse-longitudinal splitting for the exciton band, $\alpha = \hbar \omega_0 / M$, where M is the effective exciton mass. Fields φ_i and $\mathbf{P}_i$ should satisfy Maxwell boundary conditions and additional boundary conditions that will be chosen in the form of the zero exciton polarization at the boundary of the inclusion, allowing the exciton to reflect elastically from the interface.[14]

$$\varphi_1|_{r=R} = \varphi_2|_{r=R}, \tag{5}$$

$$\left(\varepsilon_\infty \frac{\partial \varphi_1}{\partial r} - 4\pi P_{1r} \right)\Big|_{r=R} = \left(\frac{\partial \varphi_2}{\partial r} - 4\pi P_{2r} \right)\Big|_{r=R}, \tag{6}$$

$$\mathbf{P}_1|_{r=R} = 0. \tag{7}$$

Solutions of the system of Eqs. (1) and (2) in the infinite crystal describe longitudinal and transverse exciton waves neglecting the retardation. They are found by expanding the electric field potential and polarization vector into a series of spherical harmonics:

$$\phi_1 = \sum_{lm} \left[c_{lm}^{(0)} j_l(\kappa r) + c_{lm}^{(1)} (r/R)^l \right] Y_{lm}(\theta\phi), \tag{8}$$

$$\begin{aligned} \mathbf{P}_1 = -\nabla \sum_{lm} & \left[d_{lm}^{(0)} j_l(\kappa r) + d_{lm}^{(1)} (r/R)^l \right] Y_{lm}(\theta\phi) \\ & + i \sum_{lm} d_{lm}^{(2)} \mathrm{curl}\left(j_l(kr) \mathbf{L} Y_{lm}(\theta\phi) \right) \\ & + \sum_{l,m} f_{lm} j_l(kr) \mathbf{L} Y_{lm}(\theta\phi), \end{aligned} \tag{9}$$

$$\phi_2 = \sum_{lm} a_{lm} (R/r)^{l+1} Y_{lm}(\theta, \phi), \tag{10}$$

$$\mathbf{P}_2 = -\nabla \sum_{lm} b_{lm}^{(1)} (R/r)^{l+1} Y_{lm}(\theta\phi), \tag{11}$$

where $\mathbf{L} = -i[\mathbf{r} \times \nabla]$, $j_l(x)$ are the spherical Bessel functions, $Y_{l,m}$ are the spherical harmonics, $k = [(\omega^2 - \omega_0^2)/\alpha]^{1/2}$ is the wave vector of the transverse waves in the infinite crystal, and $\kappa = [(\omega^2 - \omega_0^2 - 2\omega_0 \omega_{\mathrm{LT}})/\alpha]^{1/2}$ is the wave vector of the longitudinal waves in the infinite crystal. Different types of excitations that would exist in the infinite bulk crystal are coupled by the scattering and mutual transformations of the inclusion boundaries. Expansion coefficients $a_{lm} b_{lm}, c_{lm}^{(01)}, d_{lm}^{(0,1,2)}, f_{lm}$ describe a share of the particular excitation type in the eigenstates of the inclusion. Thus coefficients $a_{lm} b_{lm}, c_{lm}^{(1)}, d_{lm}^{(1)}$ stand for the contribution of the longitudinal excitations that exist in the absence of spatial dispersion ($M \to \infty$) coefficients, $c_{lm}^{(0)} d_{lm}^{(0)}$ belong to the longitudinal excitations taking into account the spatial dispersion coefficients, and $c_{lm}^{(0)}$, $d_{lm}^{(0)}, f_{lm}$ describe the transverse excitation.

Let us assume that the time dependence of the coefficients takes the form $\exp(-i\omega t)$. Then the frequencies of the eigenstates and the relationship between the coefficients can be found from the solution of the system of Eqs. (1)–(4) taking into account the boundary conditions given by Eqs. (5)–(7) by means of the expansion of Eqs. (8)–(11).

Let us present the spectrum of the solutions. There are two classes of eigenstates of the system with frequencies that may be found from the following equations:

(i) $$j_l(kR) = 0. \tag{12}$$

For this solution, all coefficients in Eqs. (8)–(11) except f_{lm} are equal to zero. These states are pure transverse excitation, do not contain an electric field, do not interact with electromagnetic waves, and therefore will not be considered further in this work.

(ii)

$$\varepsilon_\infty l+\varepsilon_2(l+1)$$

$$=4\pi\beta l\frac{\varepsilon_\infty R(\partial j_l(\kappa R)/\partial R)+\varepsilon_2(l+1)j_l(\kappa R)S_l(\kappa R)}{\varepsilon_\infty(\omega^2-\omega_0^2)D_l(\kappa k,R)}, \tag{13}$$

where

$$D_l(\kappa k,R)=R\frac{\partial j_l(\kappa R)}{\partial R}\frac{\partial}{\partial R}[Rj_l(kR)]-l(l+1)j_l(\kappa)j_l(kR), \tag{14}$$

$$\varepsilon_2=1-\omega_p^2/\omega^2, \tag{15}$$

$\omega_p=(4\pi e^2n/m)^{1/2}$ is the plasma frequency of the metal,

$$S_l(x)=x\frac{dj_l(x)}{dx}-lj_l(x). \tag{16}$$

All coefficients of the same multipole order are related to a_{lm} in the following manner:

$$c_{lm}^{(0)}=-\frac{\varepsilon_2(l+1)+\varepsilon_0 l}{\varepsilon_0 S_l(\kappa R)}a_{lm}, \tag{17}$$

$$c_{lm}^{(1)}=\left(1+\frac{\varepsilon_2(l+1)+\varepsilon_0 l}{\varepsilon_0 S_l(\kappa R)}j_l(\kappa R)\right)a_{lm}, \tag{18}$$

$$d_{lm}^{(0)}=\frac{\varepsilon_2(l+1)+\varepsilon_0 l}{4\pi\varepsilon_0 S_l(\kappa R)}a_{lm}, \tag{19}$$

$$d_{lm}^{(1)}=\frac{\beta}{\omega_0^2-\omega^2}\left(1+\frac{\varepsilon_2(l+1)+\varepsilon_0 l}{\varepsilon_0 S_l(\kappa R)}j_l(\kappa R)\right)a_{lm}, \tag{20}$$

$$d_{lm}^{(2)}=-\frac{\varepsilon_2(l+1)+\varepsilon_0 l}{4\pi\varepsilon_0 S_l(kR)}a_{lm}, \tag{21}$$

$$f_{lm}=0, \tag{22}$$

$$b_{lm}=-\frac{\omega_p^2}{4\pi\omega^2}a_{lm}. \tag{23}$$

Detailed calculations and analysis of the spectrum of excitations will be presented in the next sections.

III. OPTICAL PROPERTIES OF A METAL WITH PRECIPITATES

Optical spectroscopy is one of the methods to study electronic excitations localized on the precipitates. Determination of the optical properties of precipitates is based on the solution of the problem of light scattering by a spherical inclusion in the metal matrix. Let us consider scattering of a plane electromagnetic wave $\mathbf{E}=\mathbf{E}_0\exp(i\mathbf{kr}-i\omega t)$ by a spherical inclusion. The system is described by a set of Maxwell equations and the Schrödinger equation for the exciton polarization. These equations are more general than the set of equations used to determine the spectrum of excitations and take into account the retardation and damping of the electromagnetic waves. Inside the dielectric inclusion with spatial dispersion, electromagnetic and polarization fields are described as

$$\Delta\mathbf{E}_1-\boldsymbol{\nabla}\,\mathrm{div}\,\mathbf{E}_1+\frac{\omega^2}{c^2}\varepsilon_\infty=-\frac{4\pi\omega^2}{c^2}\mathbf{P}_1, \tag{24}$$

$$\mathbf{H}_1=-\frac{ic}{\omega}\mathrm{rot}\,\mathbf{E}_1, \tag{25}$$

$$\mathrm{div}(\varepsilon_\infty\mathbf{E}_1+4\pi\mathbf{P}_1)=0, \tag{26}$$

$$\hbar(\omega-\omega_0+i\Gamma_{\mathrm{in}}/2)\mathbf{P}_1+\frac{\hbar^2}{2M}\Delta\mathbf{P}_1=-\frac{\beta}{2\omega}\mathbf{E}_1, \tag{27}$$

where Γ_{in} is the damping constant of the material of inclusion.

For the bulk crystal, solutions of the system of Eqs. (24)–(27) are superpositions of the plane waves, two of which are transverse and one of which is longitudinal.

Outside of the dielectric inclusion, the system is described with the Maxwell equation and Drude polarization for the electron gas, taking into account the damping given by a constant Γ_m. Boundary equations are usual boundary condition of the electrodynamics (continuity of the normal component of electric induction and tangent components of the electric and magnetic fields). Additional boundary conditions for the exciton polarization have been chosen as in Eq. (7).

Solutions of Eqs. (24)–(27) have been found by expanding fields into spherical harmonics similar to the procedure used for the determination of the spectrum of excitations but assuming an incident external electromagnetic wave. Knowing the coefficients of the expansion, the cross section of the scattering can be determined. Since the size of crystallized precipitates is much less than the wavelength of the electromagnetic field, the dipole term (transverse magnetic **E** waves, $l=1$) in the scattering is dominant. As a result, the polarizability of the dielectric sphere equals

$$\alpha_{\mathrm{in}}(R)=\alpha_{\mathrm{in}}=-R^3\frac{Ak_1^2-B/2q_2^2R(\partial/\partial R)\ln(rj_1(k_1R))}{Ak_1^2+Bq_2^2R(\partial/\partial R)\ln(rj_1(k_1R))}, \tag{28}$$

where $q_2=\sqrt{\varepsilon_2}\omega/c$,

$$A=1-\frac{\alpha_1}{\alpha_2}\frac{k_2^2}{k_1^2}F(R), \tag{29}$$

$$B=1-\frac{\alpha_1}{\alpha_2}F(R)-\frac{\alpha_1}{\alpha_0}[1-F(R)], \tag{30}$$

$$F(R)=\frac{2-R^2(\partial/\partial R)\ln(Rj_1(k_1R))(\partial/\partial R)\ln(Rj_1(k_0R))}{2-R^2(\partial/\partial R)\ln(Rj_1(k_2R))(\partial/\partial R)\ln(Rj_1(k_0R))}, \tag{31}$$

$$k_0^2=\frac{2M}{\hbar}(\omega-\omega_0-\omega_{LT}+i\Gamma_{in}/2). \tag{32}$$

k_1 and k_2 are the roots of the biquadratic equation,

TABLE I. Phenomenological parameters of rare-gas crystals.

	Xe	Kr	Ar	Ne
$\hbar\omega_0$	8.36	10.19	12.06	17.36
$\hbar\omega_{\mathrm{LT}}$	0.11	0.12	0.15	0.2
M	2.2	2.2	2.2	2.2
ε_∞	2.22	1.882	1.66	1.24

$$k^4-\left(\frac{2M}{\hbar}(\omega-\omega_0+i\Gamma_{\mathrm{in}}/2)+\varepsilon_\infty\frac{\omega^2}{c^2}\right)k^2+\varepsilon_\infty\frac{\omega^2}{c^2}k_0^2=0. \tag{33}$$

Solutions of this equation determine the wave vectors of the mixed electromagnetic and exciton waves (polaritons) in the infinite crystal. Index $j=0$ corresponds to the longitudinal wave while indices $j=1,2$ enumerate two types of the transverse exciton waves.

$\alpha_j(j=0,1,2)$ are defined as

$$\alpha_j=\frac{\varepsilon_\infty}{4\pi}\frac{\hbar\omega_{\mathrm{LT}}}{\hbar^2k_j^2/2M+\hbar\omega_0-\hbar\omega-i\hbar\Gamma_{\mathrm{in}}/2}. \tag{34}$$

Polarizability of the spheric inclusion given by Eq. (28) can be used to find the dielectric constant of the metal with a system of spheric precipitates. In our calculations, we used the Lorentz-Lorenz formula for the effective dielectric function, which in our case reads

$$\varepsilon=\varepsilon_2\left(1+\frac{4\pi N\alpha_{\mathrm{in}}}{1-4\pi N\alpha_{\mathrm{in}}/3}\right), \tag{35}$$

where N is the concentration of the precipitates.

Knowing the dielectric constant, the coefficients of reflection have been calculated.

IV. CALCULATIONS AND DISCUSSION

Energy and optical spectra were calculated for the precipitates of different rare gases in aluminum. Aluminum was chosen because its plasma frequency is 15 eV and therefore the localized surface plasmon has a frequency close to the frequencies of the exciton band of the material of the inclusion. Moreover, aluminum has relatively small damping in the frequency range of interest.

Required parameters of the rare-gas precipitates of small size are mainly unknown and have to be determined experimentally. To perform the calculations, the parameters of the respective bulk rare-gas crystals were taken. Exciton states of the bulk rare crystals were studied in a large number of papers. A review of these studies can be found in Ref. 15. Parameters used for the following calculations are given in Table I. High-density effects on the crystal lattice of the precipitates were neglected in our approach.

Let us analyze the spectrum of the elementary excitations of rare-gas precipitates in aluminum given by Eq. (13). First let us consider the case of the absence of spatial dispersion. Mathematically, this corresponds to the limit $M\to\infty$ when Eq. (13) is reduced to

$$(l+1)\varepsilon_2+l\varepsilon_1=0, \tag{36}$$

where ε_1 is the dielectric constant of precipitate materials in the case of the absence of spatial dispersion,

$$\varepsilon_1=\varepsilon_\infty+\frac{4\pi\beta}{\omega_0^2-\omega^2}. \tag{37}$$

Equation (36) is the well-known formula that determines the frequencies of the polariton excitations localized on the spherical inclusion in the crystal. If a dielectric inclusion with positive dielectric constant ε_1 is embedded into a metal with negative dielectric function ε_2 given by Eq. (15), the system has a collective excitation localized in the metal outside the inclusion. It is called the localized or surface plasmon and its frequency is determined by

$$\omega_{\mathrm{spl}}=\omega_p\sqrt{\frac{2}{3+2\varepsilon_1}}. \tag{38}$$

In the region where the inclusion's dielectric function given by Eq. (37) is negative (i.e., where $\omega_0<\omega<\omega_0+\omega_{\mathrm{LT}}$) and the inclusion is surrounded by a medium with positive dielectric constant ε_2, a surface polariton state appears with the frequency given by

$$\omega_{\mathrm{spol}}=\omega_0+\frac{\varepsilon_\infty}{\varepsilon_\infty+2\varepsilon_2}\omega_{\mathrm{LT}}. \tag{39}$$

States of this kind are often observed for the semiconductor inclusions in a dielectric matrix, for example CuCl inclusions in glass.

A unique feature of the considered system of rare-gas precipitates in aluminum is the fact that the frequencies of the surface plasmon and the surface polaritons are situated close to each other. The energy of the surface plasmon excitations is in the region of about 12 eV, which is close to the energy of the lowest exciton band of a number of rare-gas crystals. This fact manifests itself in a number of remarkable effects in the energy spectrum and optical properties of the system. Figure 1 shows schematically the dependence of the position of the energy of the surface plasmons and polaritons on the value of the frequency of the bottom of the exciton band ω_0 for the oscillations with $l=1$, which interact strongly with light, calculated by solving Eq. (36). Positions of the bottom of the exciton band for the real rare-gas crystals are shown for reference. In the case where the frequency of the bottom of the exciton band is either low or high, one can clearly distinguish the levels of the excitations inside the inclusion (surface polaritons) and outside it (localized plasmons). If these levels are close, there exists strong resonant interaction between the excitation modes of the inclusion and the localized plasmons. This interaction leads to a shift of the bands and to an essential change of their intensity. Frequency shift is proportional to $\sqrt{\omega_p\omega_{\mathrm{LT}}}$. Since for aluminum $\hbar\omega_p\sim 15$ eV and for the rare-gas crystals $\hbar\omega_{\mathrm{LT}}\sim 0.1$ eV, the shift of the energy levels may be up to 1 eV.

Therefore, the shift of the energy levels in the considered system is large and exceeds by far the value of the longitudinal-transverse splitting. As the data on the effect of high pressure on the positions of the bottom of the exciton band for Ne, Ar, and Xe bubbles in Al suggest,[16] one can

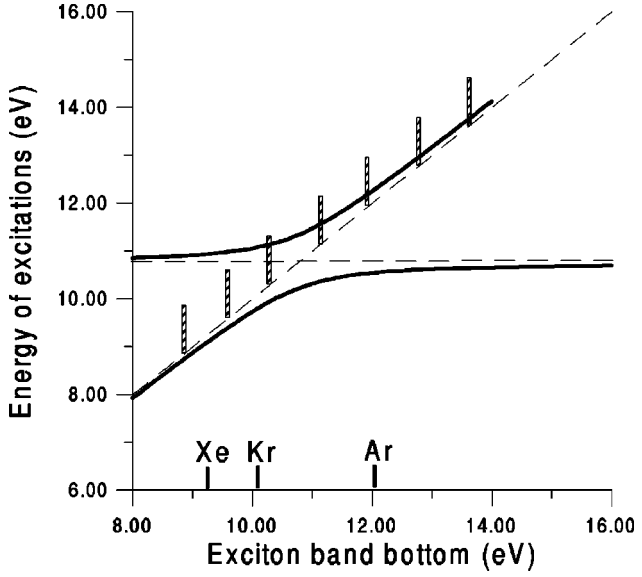

FIG. 1. Dependence of the position of the levels of the surface polaritons and the surface plasmons for the spherical inclusion in aluminum on the energy of the bottom of the exciton band of the material of inclusion. The hatched regions correspond to the exciton bands of the bulk material. The energies of the bottom of the exciton band for different rare-gas crystals are shown along the *x* axis.

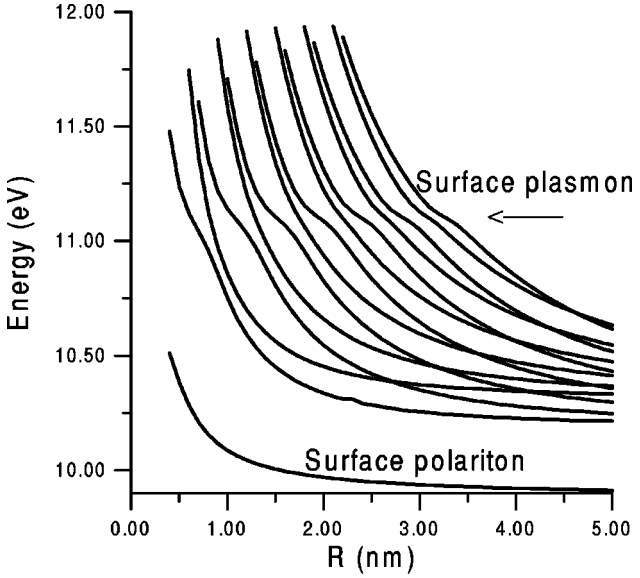

FIG. 2. Radius dependence of the position of the levels of size quantization for the Kr precipitate in Al . Arrows show the positions of the localized excitons and the localized plasmons.

expect that the considered shift is larger that the high-pressure-induced shift for the small-size precipitates.

Let us consider qualitatively effects that arise due to the finite value of the exciton bandwidth. Hatched regions in Fig. 1 (the region of energies $E>\hbar\omega_0$) correspond to the continuous spectrum of bulk excitons. For the large-size precipitates ($R\geqslant 5$ nm), the effect of the size quantization is not significant and the spectrum consists of the quasidiscrete set of states that are situated in the hatched regions in Fig. 1 depicting the levels of the surface polaritons and localized plasmons. For Ar and Ne in Al, the levels of the surface polaritons are inside the region of the quasicontinuous spectrum and are mixed with exciton levels there. As will be shown, this results in a broadening of the lines of the optical spectra. This kind of behavior is characteristic of semiconductor quantum dots in glass. For Xe and Kr, the levels of the surface polaritons are pushed outside the exciton band (due to the negative value of the dielectric constant of metal) and the above mechanism of broadening is absent.

As the size of the precipitates becomes smaller, the spectrum of the excitations acquires a more pronounced discrete character. For very small precipitates, the distance between the excitations in the energy spectrum is large. The first of the lines that is most intense in the optical spectra is shifted to higher frequencies with respect to the bottom of the exciton band of the bulk rare-gas crystal. This phenomenon interferes with mixing with the localized plasmon. If the blue-shift due to quantization (the exciton states are squeezed) makes the levels closer to the level of the localized surface plasmon, then the mixing is stronger and the position of the local plasmon is shifted more. If the frequency of the local plasmon is below the exciton bottom energy for bulk crystallite, quantization increases the distance to the local plasmon and mixing becomes weaker.

The spectrum of the size quantization of excitons in the precipitate is shown in Fig. 2 for Kr crystal as an example. The figure shows the radius dependence of the spectrum. The pressure effects are not taken into account. The spectrum displays the following remarkable features.

(i) The level of the surface polariton is lowest in the considered system.

(ii) With decreasing the radius of the precipitate, levels move to larger energies. The same displacement, though significantly less, occurs for the level of the surface polariton. In the case of the narrow band $M\rightarrow\infty$, the position of this level does not depend on the radius.

(iii) For small radii, all levels including the level of the surface polariton are situated above the exciton band bottom.

(iv) The levels of the discrete spectrum in the region of the surface-plasmon frequency interact with the plasmon. This interaction leads to an increase of the intensity of their excitation.

Figures 3–6 show the results of the calculations of the reflection spectra of ultraviolet light from the aluminum crystal containing precipitates of Ne, Ar, Xe, and Kr for different values of the exciton damping constant: (a) $\Gamma_{\text{in}}=0.1$ eV, (b) $\Gamma_{\text{in}}=0.01$ eV. For the aluminum matrix, the damping $\Gamma_m=0.1$ eV in all cases. Calculations were performed for the inclusions with radius $R=2.5$ nm for the volume share of the precipitates in the metal $\delta=0.01$ ($\delta=4\pi NR^3/3$, where N is the concentration of the inclusions). Besides the reflection spectra of the metal with precipitates (solid lines), the dashed lines in part (a) of the figures show the reflection spectra for the case when the spatial dispersion is not taken into account ($M\rightarrow\infty$).

As the exciton bands are in the region of the total internal reflection ($\omega_0<\omega_p$), they are seen in the reflection spectra as dips (with the exception of Ne precipitates, for which $\omega_0>\omega_p$). One can observe a strong dependence of the intensity of the bands (depth of the dips) on the position of the values of the bottom of the exciton band with respect to the localized plasmon frequency. This effect is due to the mixing of the exciton and plasmon states and the transfer of the oscil-

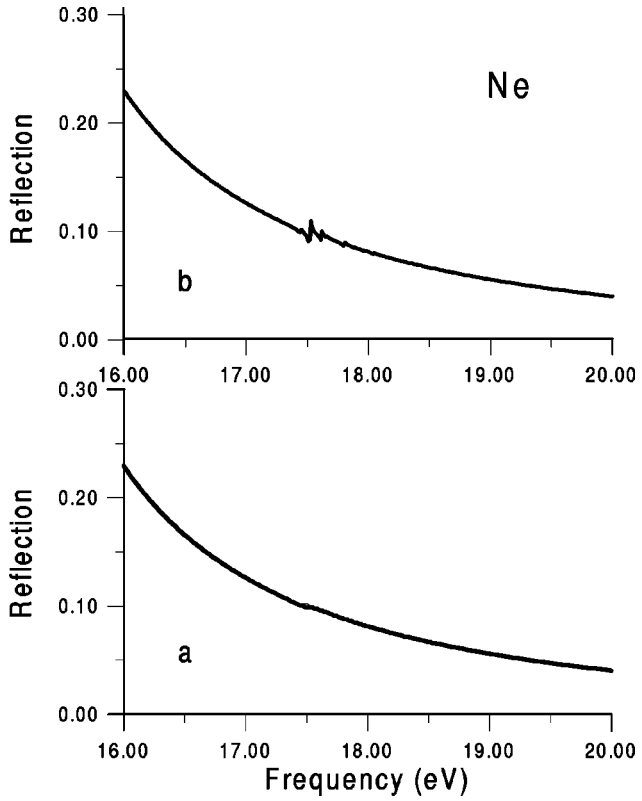

FIG. 3. Optical reflection spectra of Al with Ne precipitates. $R=2.5$ nm, $\delta=0.01$ damping, $\Gamma_m=0.1$ eV for the matrix for the precipitate $\Gamma_{in}=0.1$ eV in the case (a) and $\Gamma_{in}=0.01$ eV for the case (b).

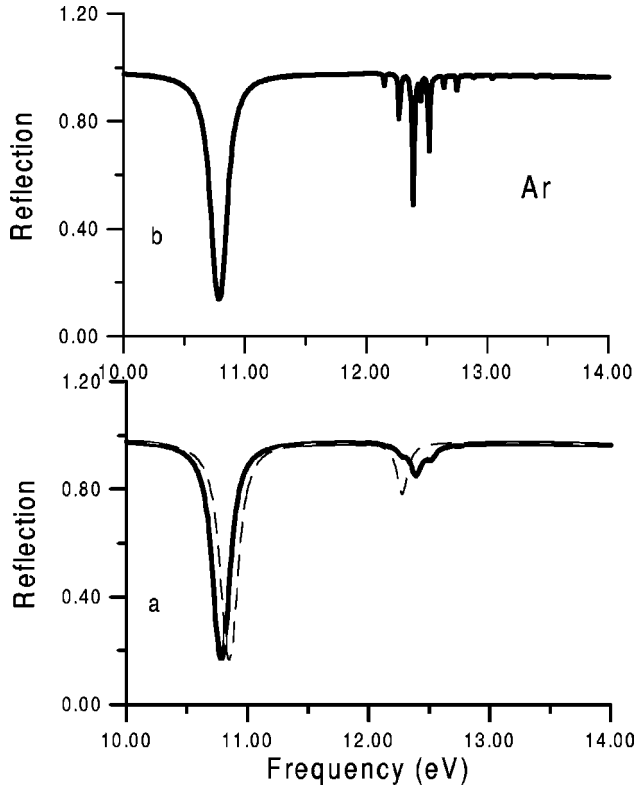

FIG. 4. Optical reflection spectra of Al with Ar precipitates. $R=2.5$ nm, $\delta=0.01$ damping, $\Gamma_m=0.1$ eV, $\Gamma_{in}=0.1$ eV in the case (a) and $\Gamma_{in}=0.01$ eV for the case (b).

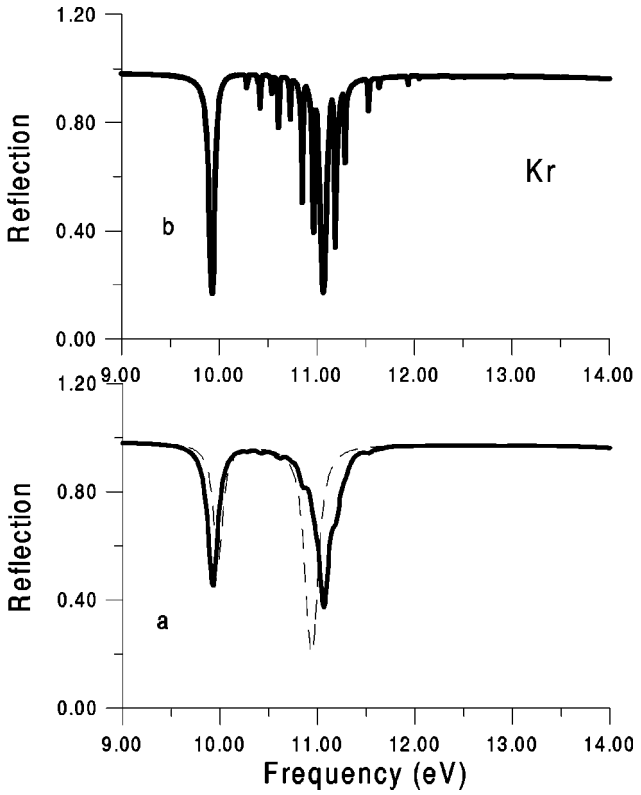

FIG. 5. Optical reflection spectra of Al with Kr precipitates. $R=2.5$ nm, $\delta=0.01$ damping, $\Gamma_m=0.1$ eV, $\Gamma_{in}=0.1$ eV in the case (a) and $\Gamma_{in}=0.01$ eV for the case (b).

lator strength from surface plasmons to excitons. The spectra of Al with Kr and Ar show the deepest dips (Fig. 4 and Fig. 5). Ne precipitates manifest themselves in the reflection spectra very weakly (Fig. 3) since the exciton band is very far from the position of the surface-plasmon level. Additionally, it is quite close to the frequency of the bulk-plasmon level interaction, with which damping increases.

The levels of the discrete spectrum are mixed with the level of the surface polariton (for Ar) or the surface plasmon (for Xe and Kr). Those discrete levels that are closest to the level of either the surface polariton or the surface plasmon manifest themselves most strongly. For the very-small-radius precipitates, the spectrum of the excitations deforms and the lowest discrete level is most prominent. In real conditions due to different reasons (scatter of the precipitate radii, etc.), the fine structure of the discrete levels would diffuse. According to Figs. 3–5, strong mixing of the discrete levels and the polariton states occurs in the region of several tenths of an eV, therefore the broadening of the spectrum will have the same order. However, for the Xe and Kr precipitates, the level of the surface polariton is pushed out of the exciton band and its position depends weakly on the radius of inclusion. Therefore, this mechanism of broadening does not apply and the surface polariton spectral line should be narrow (see the lowest-frequency band in Figs. 5 and 6).

Naturally, the discrete structure should be smoothed out by the dispersion of the radii of the inclusions and other factors. The distribution of the radii of the precipitates depends on the procedure of preparation of the sample and is not known. In Ref. 10 calculations of the dielectric function of Al with He precipitates is carried out assuming Gaussian

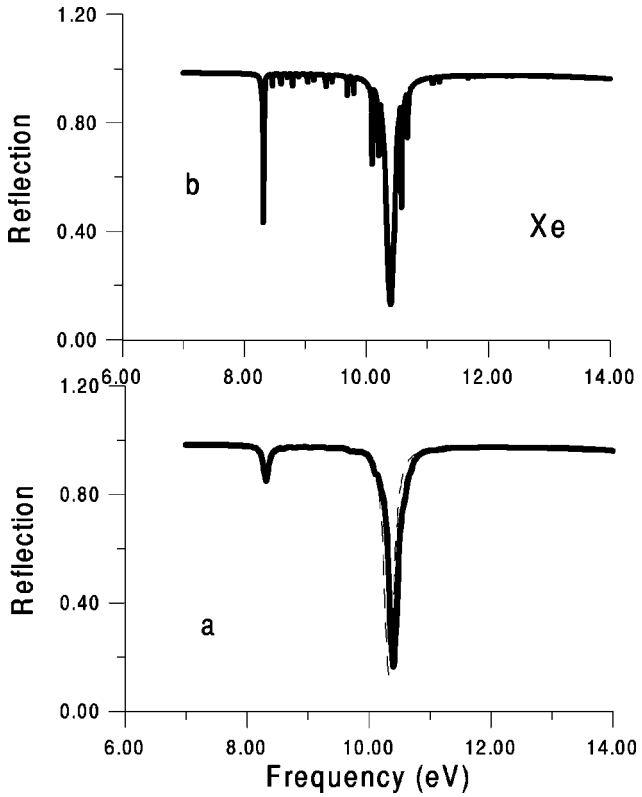

FIG. 6. Optical reflection spectra of Al with Xe precipitates. $R=2.5$ nm, $\delta=0.01$ damping, $\Gamma_m=0.1$ eV, $\Gamma_{in}=0.1$ eV in the case (a) and $\Gamma_{in}=0.01$ eV for the case (b).

distribution. It is shown that for the small inclusion radii, discrete structure can manifest itself for quite large dispersion ΔR of the radius distribution [for $R=1.0$ nm the structure is observable for $\Delta R/R\sim(0.1–0.2)R$]. A similar effect of the dispersion should be expected for the Ne, Ar, and Kr precipitates considered here.

It would be interesting to compare the conclusions of our theory with experiment. The only existing study of the optical spectra of the rare-gas bubbles in metals known to us is the measurements of the absorption spectra of Al with He bubbles.[9] Application of our theory to this system is hardly justified, however, as there is no direct confirmation of the crystallinity of He in the bubbles. Additionally, as the lowest exciton level of He is situated significantly higher than the level of the localized plasmons, the main conclusion of this paper about the strong mixing of the plasmon and exciton states is not as pronounced as for other rare-gas precipitates, though the mixing results in the blueshift of the absorption bands, which was observed in Ref. 9. Quantitative explanation of the very large value of the blueshift observed in Ref. 9 from the viewpoint of the proposed theory requires besides the crystallinity of He in bubbles, the validity of either the suggestion that most of the He atoms are concentrated in the small bubbles or rather clusters with radius less than 10 Å, or, alternatively, a suggestion about the small value of the exciton mass (less than the mass of the free electron).

Note that this work studies the lowest-energy states of the exciton series of rare-gas crystals that can be considered as Frenkel excitons. The strong resonant interaction between the higher-energy states of the exciton series, which should be considered Vannier-Mott excitons,[15] and the matrix excitations requires a separate investigation. But since the oscillator strength of the transitions decreases with the number of the excitation in the series, the effect of the resonant interaction with metal electrons should decrease as well.

V. CONCLUSIONS

The precipitates of the rare-gas atoms in metals lead to the appearance of the remarkable features in the optical properties of such metals. Strong mixing of the precipitate excitations and localized plasmons results in a gigantic shift of the positions of the reflection and absorption spectrum bands, a significant increase of the intensity of the excitations close to the frequency of the localized plasmons, and a strong redistribution of the position and the intensity of the levels of the quantized exciton spectrum of the precipitate.

The considered system may have a potential application for novel and future devices working in an ultraviolet spectral region. Study of optical spectra of metals with rare-gas precipitates can reveal useful information about the behavior of the rare-gas crystals at high pressure and temperature as well as about the phase transitions in nanostructures.[17–19]

ACKNOWLEDGMENTS

The authors would like to thank Dr. Yu.V. Kryuchenko for useful contributions and discussions.

[1] E.L. Ivchenko and G.E. Pikus, *Superlattices and Other Heterostructures* (Springer-Verlag, Berlin, 1995).
[2] Y. Kamenitsu, Semicond. Semimet. **49**, 157 (1998).
[3] V.N. Chernikov, W. Kosternich, and H. Ullmaire, J. Nucl. Mater. **227**, 157 (1996).
[4] J.H. Evans and D.J. Mazey, J. Phys. F **15**, L1 (1985).
[5] W. Jager *et al.*, J. Nucl. Mater. **111/112**, 674 (1982).
[6] D.I. Potter and C.J. Rossouw, J. Nucl. Mater. **161**, 124 (1989).
[7] K. Mitsuishi, M. Kawasaki, M. Takeguchi, and K. Furuya, Phys. Rev. Lett. **82**, 3082 (1999).
[8] S.E. Donnelly, A.A. Lucas, and J.P. Vigneron, Radiat. Eff. **78**, 337 (1983).
[9] S.E. Donnely, J.C. Rife, J.M. Gilles, and A.A. Lucas, J. Nucl. Mater. **93/94**, 767 (1980).
[10] I.Yu. Goliney and V.I. Sugakov, Fiz. Nizk. Temp. **11**, 775 (1985).
[11] A.I. Yekimov, A.A. Onushchenko, M.E. Raikh, and Al.L. Efros, Zh. Éksp. Teor. Fiz. **90**, 1795 (1986) [Sov. Phys. JETP **63**, 1054 (1986)].
[12] I.Yu. Goliney and V.I. Sugakov, Ukr. Fiz. Zh. (Russ. Ed.) **33**, 222 (1988).
[13] J.J. Hopfield and D.G. Tomas, Phys. Rev. **132**, 563 (1963).
[14] S.I. Pekar, Zh. Éksp. Teor. Fiz. **33**, 1022 (1957) [Sov. Phys. JETP

6, 758 (1958)].
[15] *Kriokristaly*, edited by B.I. Verkiv and A.F. Prikhotko Kiev (Naukova Dumka, Kiev, 1983) (in Russian).
[16] A. von Felde and J. Fink *et al.*, Phys. Rev. Lett. **53**, 922 (1984).
[17] H.H. Andersen and E. Johnson, Nucl. Instrum. Methods Phys. Res. B **106**, 480 (1995).
[18] Q. Jiang and F.G. Shi, Mater. Lett. **37**, 79 (1998).
[19] M. Awaji, N. Ishikawa, and K. Furuya, Nanostruct. Mater. **8**, 899 (1997).